Identification of Polyproline II Regions Derived From the Proline-Rich Nuclear Receptor Coactivators PNRC and PNRC2: New Insights for ERα Coactivator Interactions

C. BYRNE,[1,2,†] E. MICLET,[1,†] I. BROUTIN,[3] D. GALLO,[4] V. PELEKANOU,[5,6] M. KAMPA,[6] E. CASTANAS,[6] G. LECLERCQ,[7] AND Y. JACQUOT[1,2*]

[1]*Laboratoire des BioMolécules (LBM), CNRS - UMR 7203, Ecole Normale Supérieure / Université Pierre et Marie Curie, 24, rue Lhomond, 75231 Paris Cedex 05, France*

[2]*Fondation Pierre-Gilles de Gennes pour la Recherche, 29, rue d'Ulm, 75005 Paris, France*

[3]*Laboratoire de Cristallographie et RMN biologiques, CNRS – UMR 8015, Université Paris-Descartes, 4, avenue de l'Observatoire, 75006 Paris, France*

[4]*Service des Industries Biochimiques, Institut Meurice, avenue Emile Gryzon 1, Brussels, Belgium*

[5]*Laboratory of Pathology, University of Crete, School of Medicine, Heraklion, Greece*

[6]*Laboratory of Experimental Endocrinology, University of Crete, School of Medicine, P.O. Box 2208, Heraklion 71003, Greece*

[7]*Laboratoire J.-C. Heuson de Cancérologie Mammaire, Université Libre de Bruxelles (U.L.B.), Institut Jules Bordet, rue Héger-Bordet 1, Brussels 1000, Belgium*

ABSTRACT Protein–protein interactions are crucial for signal transductions required for cell differentiation and proliferation. Their modulation is therefore key to the development of therapeutic alternatives, particularly in the context of cancer. According to literature data, the polyproline-rich nuclear receptor coactivators PNRC and PNRC2 interact with estrogen receptor (ERα) through their PxxP SH3-binding motifs. In a search to identify the molecular features governing this interaction, we explored using electronic circular dichroism (ECD) spectroscopy and molecular dynamics (MD) calculations, the capacity of a range of putative biologically active peptides derived from these proteins and containing this PxxP motif(s) to form polyproline II (PPII) domains. An additional more exhaustive structural study on a lead PPII peptide was also performed using 2D nuclear magnetic resonance (NMR) spectroscopy. With the exception of one of all the investigated peptides (PNRC-D), binding assays failed to detect any affinity for Grb2 SH3 domains, suggesting that PPII motifs issued from Grb2 antagonists have a binding mode distinct from those derived from Grb2 agonists. Instead, the peptides revealed a competitive binding ability against a synthetic peptide (ERα17p) with a putative PPII-cognate domain located within a coregulator recruitment region of ERα (AF-2 site). Our work, which constitutes the first structure-related interaction study concerning PNRC and PNRC2, supports not only the existence of PxxP-induced PPII sequences in these coregulators, but also confirms the presence of a PPII recognition site in the AF-2 of the steroid receptor ERα, a region important for transcription regulation. *Chirality 25:628–642, 2013*.

KEY WORDS: estrogen receptor α; proline-rich nuclear receptor coactivator PNRC; polyproline II; electronic circular dichroism; NMR; molecular dynamics

INTRODUCTION

Protein–protein interactions are crucial for signal transductions required for cell differentiation and proliferation. In this context, direct modulation of the activation of the estrogen receptor α (ERα), through surface protein "platforms" involved in the recruitment of protein partners ("coregulators"), is of particular interest in the growth control of hormone-dependent breast tumors. The first approach routinely used for breast cancer treatment consists of inserting antiestrogens within the ligand-binding pocket of ERα (e.g., tamoxifen,[1] fulvestrant[2]), impeding thereby its ability to recruit protein-derived coactivators. A second proposed approach, not yet found in clinical practice, involves direct interference at the surface of the receptor to inhibit the recruitment of such coactivators. The surface domains of the ERα (called activation function AF-1 and AF-2), acting either in the absence of a ligand (AF-1, at the N-terminus of the protein), or in its presence (AF2, in the vicinity of the estradiol binding pocket) are prime targets for such a purpose.[3–5] To date, the most explored category of coactivators is characterized by an LxxLL cognate sequence(s) (where L corresponds to leucine and x to any amino-acid).[3–13] This motif mediates the formation of "receptor/ligand/coactivator" tripartite complexes, required for transcription, through targeting specific DNA regions located at promoter sites (i.e., estrogen-response elements; EREs).[7,10]

Recently, a family of coactivators referred to as the proline-rich nuclear receptor coactivator (PNRC) family has been described. Two proteins belonging to this family, PNRC and PNRC2, were reported to contain both SH3- and ERα-binding motifs (i.e., PxxP and LxxLL motifs, respectively). PNRC (327 residues, MW ~35 kDa)[14] (Scheme 1) contains two proline-rich regions that bind not only to Grb2 SH3 domains[15] but also to ERα,[16] independently from the presence of a C-terminus LxxLL motif. The protein called PNRC2 (139 residues,

Additional Supporting Information may be found in the online version of this article.

*Correspondence to: Yves Jacquot, Laboratoire des BioMolécules (LBM), CNRS – UMR 7203, Ecole Normale Supérieure, 24, rue Lhomond, 75352 Paris Cedex 05, France. E-mail: yves.jacquot@upmc.fr

†The first two authors contributed equally.

Received for publication 2 July 2012; Accepted 12 April 2013

DOI: 10.1002/chir.22188

Published online 8 August 2013 in Wiley Online Library (wileyonlinelibrary.com).

a)

```
          1                                                  50
PNRC      MTVVSVPQRE PLVLGGRLAP LGFSSRGYFG ALPMVTTAPP PLPRIPDPRA
PNRC2     .......... .......... .......... .......... ..........
Consensus .......... .......... .......... .......... ..........

          51                                                 100
PNRC      LPPTLFLPHF LGGDGPCLTP QPRAPAALPN RSLAVAGGTP RAAPKKRRKK
PNRC2     .......... .......... .......... .......... ..........
Consensus .......... .......... .......... .......... ..........

          101                                                150
PNRC      KVRASPAGQL PSRFHQYQQH RPSLEGGRSP ATGPSGAQEV PGPAAALAPS
PNRC2     .......... .......... .......... .......... ..........
Consensus .......... .......... .......... .......... ..........

          151                                                200
PNRC      PAAAAGTEGA SPDLAPLRPA APGQTPLRKE VLKSKMGKSE KIALPHGQLV
PNRC2     .......... .......... .......... .....MGGGE RYNIPAPQSR
Consensus .......... .......... .......... .....MGggE riaiPagQlr

          201                                                250
PNRC      HGIHLYEQPK INRQKSKYNL PLTKITSAKR NENNFWQDSV SSDRIQKQEK
PNRC2     NVSK..NQQQ LNRQKTKEQN SQMKIVHKKK ERGHGYNSSA AAWQAMQNGG
Consensus ngih..#Qqq iNRQKsKe#n pqmKIthaKr #rnngw#dSa aadraqq#eg

          251                                                300
PNRC      KPFKNTENIK .NSHLKKSAF LTEVSQKENY AGAKFSDPPS PSVLPKPPSH
PNRC2     KNKNFPNNQS WNSSLSGPRL LFKSQANQNY AGAKFSEPPS PSVLPKPPSH
Consensus Knknnp#Nqk .NShLkgpal Lfesqan#NY AGAKFS#PPS PSVLPKPPSH

          301                        328
PNRC      WMGSTVENSN QNRELMAVHL KTLLKVQT
PNRC2     WV..PVSFNP SDKEIMTFQL KTLLKVQV
Consensus Wm..pVennn q#rEiMafqL KTLLKVQt
```

b)

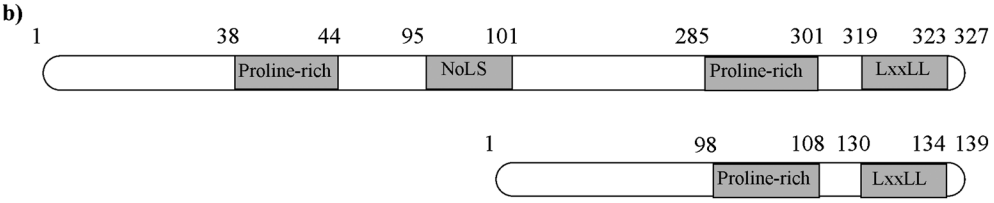

Scheme 1. (**a**) Sequence alignment[37] of the two coactivators PNRC (PNRC1_HUMAN Q12796) and PNRC2 (PNRC2_HUMAN Q9NPJ4). (**b**) Localization of the different signaling domains of PNRC and PNRC2. NoLS refers to nuclear localization signal.

MW ~16 kDa, 96% identity with PNRC, Scheme 1) differs from the former by the lack of its N-terminus tail, which contains the $A^{38}PPPLPR^{44}$ proline-rich sequence. Strikingly, this corresponds to one of the two key PxxP motifs necessary for Grb2 association.[15,17] As such, this PNRC-2 isoform fails to interact with Grb2 but binds to ERα, as does PNRC. Zhou et al. have demonstrated that mutations of the proline residues within the $P^{287}PSP^{290}$ motif of PNRC were accompanied by a dramatic decrease in the protein's affinity for ERα.[16] These observations suggest strongly that a cognate domain appropriate for PxxP association, such as SH3-like domains, might be found at the surface of the receptor. According to the same study, this domain could correspond to the H4 / type II β turn (residues 364–370) region of ERα,[16–18] which is overlapped by the 295–311 flexible sequence (end of the hinge region). It is noteworthy that the latter sequence is important in the control of estrogen receptor-induced transcription and is also in charge of the recruitment of calmodulin and Hsp70.[19–23] In such a context, it was of interest to explore the possibility of interaction with ERα of peptides issued from PNRC or PNRC2 and sharing PxxP sequences. Whether such putative association could be mediated by the stability or the extent of their polyproline II (PPII) structures is another question of interest. Such issues are addressed here.

In the current study, we present electronic circular dichroism (ECD) and 2D nuclear magnetic resonance (NMR) conformational investigations as well as molecular dynamics (MD) calculations carried out on peptides containing the proline-rich regions of both PNRC and PNRC2 (Table 1) and proposed to be important for Grb2 and ERα association.[15–17] The interaction of these peptides with Grb2 and ERα has been assessed by fluorescence spectroscopy and enzyme-linked immunosorbent assay (ELISA), respectively. Our work shows that the synthetic peptides containing the PNRC and PNRC2 PxxP proline-rich sequences adopt, to varying extents, a PPII secondary structure capable of interacting with the ligand-binding domain of ERα, and more specifically in a region located between the helices H3 and H5 (AF-2 region).

MATERIALS AND METHODS

Solid-Phase Peptide Synthesis and Purification

The peptides Ac-SDPPSPSVLPK-NH_2 (PNRC-A), Ac-SEPPSPSVLPK-NH_2 (PNRC-B), Ac-VLPKPPSHW-NH_2 (PNRC-C), Ac-APPPLPR-NH_2 (PNRC-D), Ac-SDPPSPSVLPKPPSHW-NH_2 (PNRC-E), and Ac-SEPPSPSVLPKPPSHW-NH_2 (PNRC-G) were synthesized manually or on an automated peptide synthesizer (433A Applied Biosystems, Foster City, CA) by standard Boc solid-phase peptide synthesis (SPPS) methodology, on a 0.1 mmol scale, using MBHA resin (1 eq., substitution: 1.26 mmol/g or 0.51 mmol/g, Senn Chemicals Int., Cachan, France). Dicyclohexylcarbodiimide (DCC, Applied Biosystems, Courtaboeuf, France) and 1-hydroxybenzotriazole (HOBt, Applied Biosystems,Courtaboeuf, France) both 1.0 M solutions in N-methylpyrolidone (NMP), were used to activate and couple the amino acids (10 eq., 1 mmol). Manual coupling was carried out in a fritted syringe over 30 min using 10 equivalents of HOBt/DCC in NMP with agitation. After washing with NMP, then DCM, deprotection was carried out using neat TFA (1 x 1 min, followed by 1 x 5 min). After each deprotection, the peptide chain was neutralized with diisopropylethylamine (DIPEA, 50% in dichloromethane [DCM]) and washed with NMP.

The branched peptides Ac-APPPLPRK(Ac-SPSPPDS)-NH_2 (PNRC-H) and Ac-APPPLPRK(Ac-SDPPSPS)-NH_2 (PNRC-I) were synthesized using an orthogonal protection strategy on MBHA resin preloaded with Boc-Lys(Fmoc)-OH. The resin-bound, side-chain protected linear peptide Ac-APPPLPR(Tos)K(Fmoc) was synthesized manually (0.2 mmol) in a fritted syringe using standard Boc SPPS. Coupling and deprotection was carried out as described above. After synthesis of the protected linear chain, the Fmoc side-chain protecting group was removed by agitation of the beads in piperidine (20% in NMP, 2 x 10 min). After removal of the Fmoc group, the resin was split in two. The peptide branches Ac-SPSPPDS (PNRC-H) and Ac-SDPPSPS (PNRC-I) were added by continued Boc SPPS on the lysine ϵ-amino group (0.1 mmol peptide resin).

TABLE 1. List of the synthesized peptides that have been assayed (code, sequence, residues of the corresponding regions of PNRC and PNRC2 are specified)

Code of peptides	Sequence	Residues	Protein	Localization
PNRC-A	Ac-SDPPSPSVLPK-NH_2	285 to 295	PNRC	Cter
PNRC-B	Ac-SEPPSPSVLPK-NH_2	99 to 109	PNRC2	Cter
PNRC-C	Ac-VLPKPPSHW-NH_2	292 to 300	PNRC	Cter
		102 to 114	PNRC2	Cter
PNRC-D	Ac-APPPLPR-NH_2	38 to 44	PNRC	Nter
PNRC-E	Ac-SDPPSPSVLPKPPSHW-NH_2	285 to 300	PNRC	Cter
PNRC-F	Ac-SDPPSPSVLPKPPSH-NH_2	285 to 299	PNRC	Cter
PNRC-G	Ac-SEPPSPSVLPKPPSHW-NH_2	99 to 114	PNRC2	Cter
PNRC-H	Ac-APPPLPRK(Ac-SPSPPDS)-NH_2	38 to 44	PNRC	both
		291 to 285		
PNRC-I	Ac-APPPLPRK(Ac-SDPPSPS)-NH_2	38 to 44	PNRC	both
		285 to 291		

The prolines involved in the SH3-binding signature PxxP are underlined.

Cleavage and concomitant deprotection of the protected peptide resin was carried out in HF using dimethylsufide (0.25 mL/g) and anisole (1.25 mL/g) as scavengers. The ether precipitated peptides were filtered, dissolved in degassed milliQ water: acetic acid (75: 25) and lyophilized.

The peptide PNRC-F was synthesized using Fmoc strategy due to the presence of a co-eluting impurity when synthesized using the Boc strategy. This peptide was synthesized on a 0.1 mmol scale using a Rink amide resin with a loading of 0.70 mmol/g and using HBTU/DIPEA (9.5 eq., 0.95 mmol / 2 mmol) coupling with appropriately protected Fmoc amino acids (10 eq., 1 mmol). Cleavage was carried out using TFA:TIPS:H_2O (95:2.5:2.5).

The crude products were purified by semipreparative RP-HPLC (solvent A: milliQ water / 0.1% of TFA; solvent B: 60% acetonitrile / 40% milliQ water / 0.1% TFA) on a Dionex HPLC system (Dionex P580 Pump, Dionex AD25 Absorbance Detector, Dionex 4400 Integrator) equipped with a SymmetryPrep C_8 RP-HPLC column (Waters 7.8 mm x 300 mm, 7 μm particle size, 300 Å pore size). Purification was monitored at 220 nm. The purified peptides were identified by MALDI-TOF (matrix-assisted laser desorption ionization time-of-flight) mass spectrometry (4700 Proteomic Analyzer, Applied Biosystems, Foster City, CA).

- Ac-SDPPSPSVLPK-NH_2 (PNRC-A): Rt = 12.9 min (linear gradient from 5 to 60% B for 20 min, flow rate 5 mL/min). Purity estimated by analytical RP-HPLC: > 95%. m/z = 1163.61 (M^+, calc); m/z = 1164.63 (MH^+, found).
- Ac-SEPPSPSVLPK-NH_2 (PNRC-B): Rt = 12.6 min (linear gradient from 10 to 60% B for 30 min, flow rate 5 mL/min). Purity estimated by analytical RP-HPLC: ~98%. m/z = 1177.62 (M^+, calc); m/z = 1178.64 (MH^+, found).
- Ac-VLPKPPSHW-NH_2 (PNRC-C): Rt = 16.3 min (linear gradient from 5 to 60% B for 20 min, flow rate 5 mL/min). Purity estimated by analytical RP-HPLC: ~98%. m/z = 1100.60 (M^+, calc); m/z = 1101.55 (MH^+, found).
- Ac-APPPLPR-NH_2 (PNRC-D): Rt = 17.0 min (linear gradient from 10 to 40% B for 30 min, flow rate 5 mL/min). Purity estimated by analytical RP-HPLC: ~98%. m/z = 787.46 (M^+, calc); m/z = 788.50 (MH^+, found).
- Ac-SDPPSPSVLPKPPSHW-NH_2 (PNRC-E): Rt = 9.8 min (linear gradient from 20 to 40% B for 20 min, flow rate 5 mL/min). Purity estimated by analytical RP-HPLC: >95%. m/z = 1768.90 (M^+, calc); m/z = 1769.33 (MH^+, found).
- Ac-SDPPSPSVLPKPPSH-NH_2 (PNRC-F): Rt = 8.3 min (linear gradient from 15 to 20% B for 30 min, flow rate 5 mL/min). Purity estimated by analytical RP-HPLC: >95%. m/z = 1582.37 (M^+, calc); m/z = 1582.80 (MH^+, found).
- Ac-SEPPSPSVLPKPPSHW-NH_2 (PNRC-G): Rt = 10.0 min (linear gradient from 20 to 40% B for 20 min, flow rate 5 mL/min). Purity estimated by analytical RP-HPLC: >95%. m/z = 1782.99 (M^+, calc); m/z = 1783.82 (MH^+, found).
- Ac-APPPLPRK(AcSPSPPDS)-NH_2 (PNRC-H): Rt = 8.6 – 10.6 min (linear gradient from 20 to 40% B for 20 min, flow rate 5 mL/min). Purity estimated by analytical RP-HPLC: >95%. m/z = 1625.26 (M^+, calc); m/z = 1625.80 (MH^+, found).
- Ac-APPPLPRK(AcSDPPSPS)-NH_2 (PNRC-I): Rt = 12.0 min (linear gradient from 15 to 35% B for 20 min, flow rate 5 mL/min). Purity estimated by analytical RP-HPLC: >95%. m/z = 1625.26 (M^+, calc); m/z = 1625.87 (MH^+, found).

Conformational Analysis

Electronic circular dichroism. ECD experiments were carried out to explore the conformational characteristics of the peptides. The peptides (PNRC-A, B, C, and D at 80 μM) were dissolved in a 10 mM phosphate buffer solution to achieve a final concentration of 30 μM. ECD spectra were recorded at 5 °C on a Jobin Yvon ECD6 spectropolarimeter, using a quartz cell (0.1 cm path length). Guanidine hydrochloride (GnCl, maximum concentration 7.0 M) or calcium chloride ($CaCl_2$, maximum concentration 6.0 M) were dissolved in milliQ water (18 MΩ) and were used to promote a higher proportion of PPII or to destabilize any defined conformational state, respectively, and, thereby, to assess both the propensity of the peptides to adopt a PPII conformation and, conversely, to evaluate the stability of this structure when already present.[24–29] Before acquisition, the samples were allowed to equilibrate for 5 min at 5 °C in the spectropolarimeter. Measurements were carried out over the 190–260 nm wavelength range. Each spectrum was averaged over four scans and subjected to smoothing after subtraction of the buffer background. ECD data were analyzed using the Dichrograph Software (v. 1.2). The unit of measured circular dichroism (mean residue molar circular dichroism, $\Delta\epsilon_{MR}$, $M^{-1}.cm^{-1}$) has been converted into mean residue molar ellipticity [θ], which corresponds to the molar ellipticity ($deg.dmol^{-1}.cm^2$), following the equation $[\theta]=3298\ \Delta\epsilon_{MR}$. The percentage of PPII in solution was estimated from the equation $\%PPII = \frac{[\theta]_{max} + \left|[\theta]_{CaCl_2}\right|}{[\theta]_{GnCl} + \left|[\theta]_{CaCl_2}\right|} \times 100$, where $[\theta]_{max}$ corresponds to the mean residue molar ellipticity ($deg.dmol^{-1}.cm^2$) at the characteristic maximum for PPII (i.e., at ~227 nm), where $[\theta]_{CaCl_2}$ corresponds to the mean residue molar ellipticity of PPII with high concentration of $CaCl_2$ and where $[\theta]_{GnCl}$ corresponds to the mean residue molar ellipticity of PPII with high concentration of GnCl.[25,29]

NMR experiments. NMR structural studies were performed on a Bruker Avance III spectrometer, operating at a ^1H frequency of 500 MHz and equipped with a triple resonance, z-axis pulsed-field-gradient cryogenic probehead, optimized for ^1H detection. Lyophilized PNRC-D (2 mg) was dissolved in 550 μL phosphate buffer (10 mM, pH 6.5) in H_2O:D_2O (90:10) or in 100% D_2O. DSS (4,4-dimethyl-4-silapentane-1-sulfonic acid, 1 mM) was added for proton and carbon chemical shift calibration. Complete proton assignment was obtained from the analysis of a 2D total correlation spectroscopy (TOCSY) experiment using an 80 ms DIPSI-2 mixtime,

and 2D rotating frame Overhauser effect spectroscopy (ROESY) experiments (300 ms mixing time). Homonuclear experiments were typically collected as 512 (t1) and 4096 (t2) time-domain matrices over a spectral width of 10 ppm, with 8 scans per t1 increment. Carbon assignment was deduced from heteronuclear 2D ^{1}H-^{13}C HSQC, using a 256 (t1) x 1024 (t2) time-domain matrix, with 32 scans per t1 increment. Data were processed using the TOPSPIN 2.0 software (Bruker). Shifted sine-bell window functions were applied in both indirect and direct detected dimensions and extensive zero-filling prior to Fourier transformation was used to yield high digital resolution. Spectra were analyzed using the CARA software (Computer-Aided Resonance Assignment, v. 1.2.3. http://cara.nmr.ch/doku.php).[30] Homonuclear $^{3}J_{H^{N}H^{\alpha}}$ (respectively $^{3}J_{H^{\alpha}H^{\beta}}$) vicinal couplings were directly obtained from amide resonances (respectively proline H^{α} resonances) in 1D proton spectra.

NMR structure calculation. Simulated annealing (SA) calculations were carried out with the program DYNAMO 2.1 (Delaglio F. Dynamo NMR Molecular Structure Engine, v. 2.1. http://spin.niddk.nih.gov/NMRPipe/dynamo/) and consisted of three stages.[31] The first stage comprised an initialization period of 1000 steps (3 fs long) of molecular dynamics at 4000 K and very tight temperature control. In a second stage, the coordinates were maintained at 4000 K with loose temperature control for 4000 steps. In the final stage, the structure was annealed by slowly reducing the temperature from 4000 K to 0 K over the space of 20,000 molecular dynamic steps (3 fs long). In the first two stages, force constants were set as follows: 1000 kcal.mol^{-1}.Å^{-2}, 250 kcal.mol^{-1}.rad^{-2}, 50 kcal.mol^{-1}.rad^{-2}, 2 kcal.mol^{-1}.Å^{-2} for bonds, angles, impropers, and NOE constraints, respectively. No Van der Waals interactions were operative. During the final stage, the bonds force constant was maintained at 1000 kcal.mol^{-1}.Å^{-2}, both angles and impropers to 500 kcal.mol^{-1}.rad^{-2}, the ROE term was increased exponentially from 2 to 30 kcal.mol^{-1}.Å^{-2}. The Van der Waals interactions and *J*-coupling restraints were slowly introduced during cooling to reach the final values of 4 kcal.mol^{-1}.Å^{-2} and 1 kcal.mol^{-1}.rad^{-2}, respectively.

NMR constraints consisted of 3 $^{3}J_{H^{N}H^{\alpha}}$, 8 $^{3}J_{H^{\alpha}H^{\beta}}$, 45 ROE (25 inter- and 20 intra-residues distance restraints extracted from the ROESY experiments). Additionally, 8 Φ- and Ψ-dihedral angles in proline residues were predicted from the TALOS+ software and used as constraints for the structure calculations.[32] The volumes of the ROESY cross peaks were converted into upper distance bounds of ca. 2.8, 3.8, or 5.0 Å. For each oligomer 200 structures were calculated starting from an extended fold. Typical final energies (kcal.mol^{-1}) of PNRC-D were 1.6; 6.1; 1.4; 27.4; 6.3 and 25.6 for *J*-coupling, bond, impropers, angle, NOE, and Van der Waals force constants, respectively.

Molecular dynamics (MD) studies. All MD simulations were performed using the Amber 11 software package and the ff99SB force field.[33,34] The lowest energy structure obtained on PNRC-D by simulated annealing was subjected to an MD simulation using the Born solvation model implemented in Amber. First, the peptide structure was minimized at 300 K using 500 steps with the steepest descent and 500 steps with the conjugate gradient algorithms. Second, molecular dynamics simulations were performed at constant temperature for 10 ns using 1 fs time steps. Coordinates and energies were recorded every 200 steps, allowing analyses of trajectories.

Biochemistry

Grb2 interaction assays. Recombinant Grb2 protein was produced and purified according to a previously published protocol.[35] The association of each peptide with the recombinant Grb2 protein was assessed by using fluorescence-based titration assays. The experiments were conducted at 18 °C in a stirred 1 cm pathlength cell using a Jasco FP-6200 spectrofluorimeter (Jasco, Essex, UK). Excitation and emission wavelengths were defined at λ = 280 nm and λ = 350 nm, respectively. The concentration of Grb2 was kept at 1 μM in 50 mM Tris buffer adjusted to pH 8.0. The dissociation constants (Kd) were determined by monitoring the changes of fluorescence upon the addition of 5 μL of a peptide solution at 10^{-3} M or 10^{-4} M. The experimental curves were analyzed with the Monte-Carlo based MC-Fit program.[36]

ERα interaction assays. According to our previous observations,[18] the flexible 295–311 region of the ERα adopts a mixed PPII/α-helix conformation, which is subjected to intramolecular interactions with the H4 / type II β-turn (AF-2, residues 364–370, PNRC-binding region), as shown in Figure 1a,b. A synthetic 17-mer peptide corresponding to this 295–311 region (ERα17p, H-PLMIKRSKKNSLALSLT-OH) competes with its ERα parent sequence.[19] Hence, a surface-bound biotinylated version of ERα17p appeared to us as a useful tool to detect possible competition by other peptides with the H4 / type II β-turn of the receptor, since such a peptide would logically decrease ERα binding to the matrix surface. Such an assay was performed with an indirect sandwich ELISA according to a procedure described hereafter (Fig. 1b).

The wells of an avidin-coated ELISA 96 multiwell plate (React-Bind Streptavidin High Binding Capacity Coated Plates, Thermo Scientific Pierce, Erembodegem, Belgium) were washed four times with 200 μL of buffer solution (Trisma Base 25 mM, NaCl 150 mM, pH 7.2, 0.1% BSA, 0.05% Tween-20). Biotinylated ERα17p at 5 x 10^{-5} M (200 μL) was then added (coating stage) to each well and incubated overnight at 4 °C. After washing four times with 200 μL of buffer solution, 100 μL of purified recombinant human ERα (wt 67 kDa hERα, Calbiochem, La Jolla, CA) at a concentration of 0.15 nM were added to each well in the absence (control) or in the presence of each investigated peptide. These mixtures were incubated for 1 h at room temperature with gentle stirring before washing (four times with 200 μL of buffer solution). As shown in Figure 1b, binding detection was carried out by the addition of 150 μL of the primary ERα antibody HC20 (Santa Cruz Biotechnology, Santa Cruz, CA; dilution: 1/1000; 1 h incubation with gentle stirring at room temperature followed by washing) and 200 μL of the secondary antibody (goat antirabbit) bound to horseradish peroxidase (HRP, ImmunoPure Biotinylated Horseradish Peroxydase, Pierce Thermo Scientific, Erembodegem, Belgium) in the same conditions (dilution: 1/2500). ERα measurement was performed by colorimetry and the absorbance was recorded at 450 nm in the presence of tetramethylbenzidine (TMB; Pierce Thermo Scientific, Erembodegem, Belgium).

Sequence Alignment

The sequences were downloaded from the NCBI (National Center for Biotechnology Information) website http://www.ncbi.nlm.gov/protein. The references for the primary sequences of PNRC and PNRC2 are PNRC1_HUMAN (Q12796) and PNRC2_HUMAN (Q9NPJ4), respectively. Multiple-sequence alignments were performed by using the Multalin software (http://multalin.toulouse.inra.fr/multalin/),[37] which is based on a conventional iterative and progressive algorithm method. A hierarchical clustering of the sequences was performed before alignment and the closest sequences were determined by generating aligned sequence groups. The close groups were then aligned until a unique group was created. The protein alignment algorithm Blosum 62-12-2, which is known to be the best available matrix for detecting weak protein similarities, was used for calculations.

RESULTS

Conformational Studies

ECD spectroscopy. With respect to the interaction of PNRC with Grb2 SH3 domains,[15] the synthesized PxxP-containing regions of PNRC (Table 1) may adopt a PPII secondary structure.[38] Briefly, PPII corresponds to a solvent exposed extended left-handed helix (3_1-helix) typically comprised of successive prolines; it is characterized by *trans* amide bonds, no intramolecular hydrogen bonds, three residues per turn, a pitch of 9.3 Å, and mean φ and ψ dihedral angle values of ~-75° and ~150°, respectively.[26,28,39–42] Although this conformation represents a key feature for numerous protein–protein interactions and due to the lack of

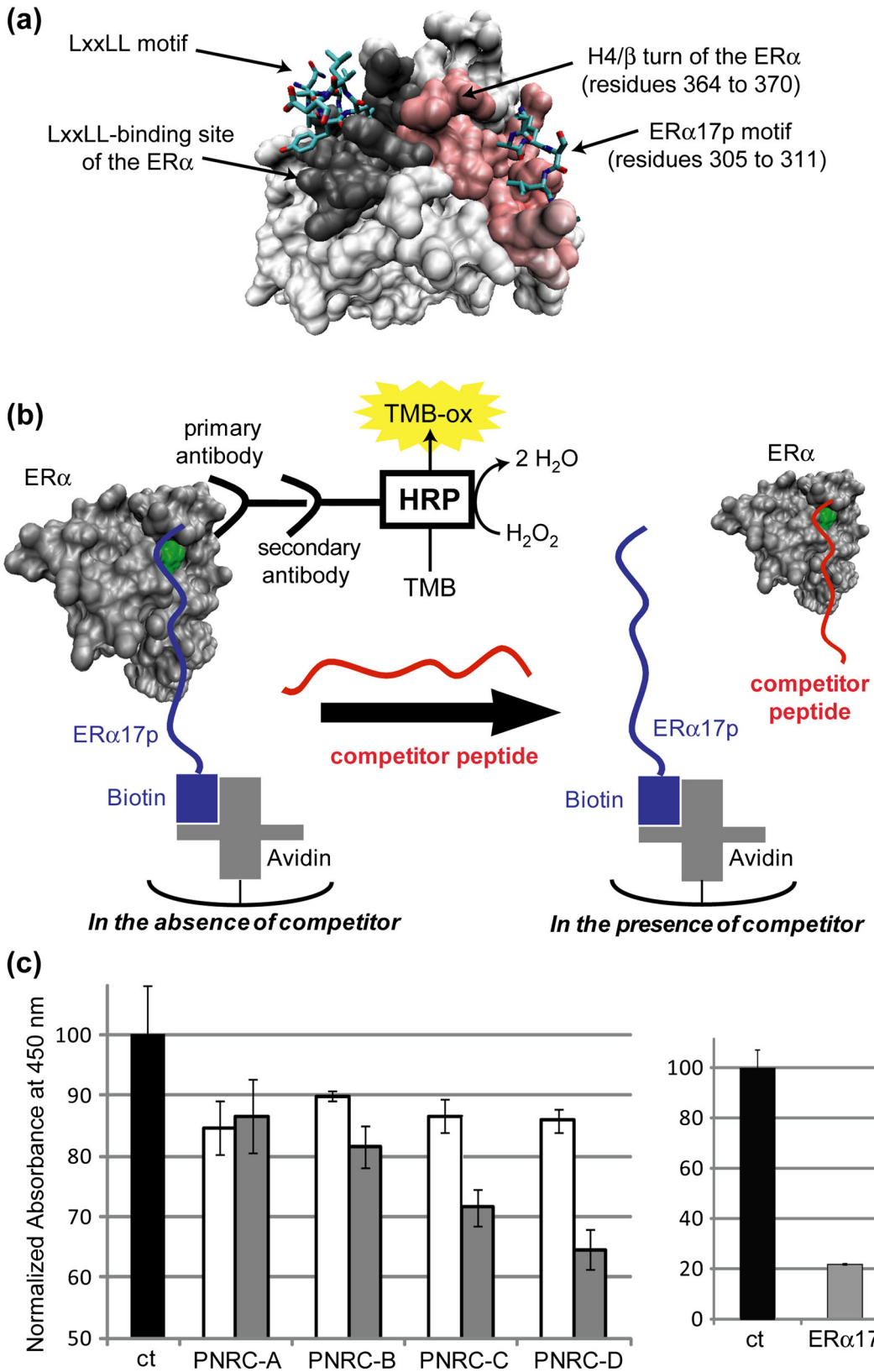

Fig. 1. (**a**) ERα-LBD Connolly surface displaying the ERα LxxLL-binding site (in gray), and the PNRC-binding site (in pink). The LxxLL and the ERα17p sequences are drawn (complex with estradiol, Worldwide Protein Data Bank (PDB code: 1GWR[91])). (**b**) Indirect sandwich ELISA. After the addition of biotinylated ERα17p (in blue) on an avidine-coated plate, purified recombinant human ERα (in gray) is added. In the absence of PNRC peptide competitor (in red), the biotinylated ERα17p retains ERα through its H4/β-turn region (in green). The interaction between ERα and bound ERα17p is recorded by addition of the primary ERα antibody HC20 and a secondary antibody linked to horseradish peroxidase (HRP), which transforms 2,2,5,5-tetramethylbenzidine (TMB) into a chromophore absorbing at 450 nm (TMB-ox). When a PNRC peptide competitor is added to this assay (in red), it occupies the H4/β-turn region, preventing the immobilization of ERα on the plate. (**c**) Inhibitory effects of PNRC-A, -B, -C, and -D at 1 μM (white bars) and 10 μM (grey bars) on the recruitment of ERα17p; data presented on the right refers to experiments in which nonbiotinylated ERα17p 10 μM was used as a positive control (data representative of an experiment performed twice in triplicate). [Color figure can be viewed in the online issue, which is available at wileyonlinelibrary.com.]

stabilizing intramolecular hydrogen bond, PPII is sometimes considered a transitory component of disordered states in proteins and peptides.[41,43–48] The CD spectral signature of PPII is characterized by a strong negative band at ~202 nm ($\pi\pi^*$ transition) and a weak positive band at ~220 nm ($n\pi^*$ transition).[26–28,49] Even if the number of proline residues corroborates with PPII stability, it relies on other parameters such as the proline position in the primary sequence, the nature and position of nonproline residues,[42,50–53] as well as the C- and N-terminus groups.[54] In this regard, it is noteworthy that peptides devoid of proline can adopt PPII structure,[55] as exemplified by acidic[27,43] and basic[43,44] residue-rich peptides or alanine-rich peptides.[46–48,56–61] Thus, it seems worthwhile to investigate the influence of the nonproline residues (and more specifically of Val, Leu, Lys, Glu, Asp) in the PPII stability of the various PNRC peptides.[51,62] The ECD spectra of the peptides PNRC-A, -B, -C, and –D, recorded between 190 and 260 nm, suggest the possible presence of PPII conformation, as outlined by a strong negative maximum at ~202 nm and a weak positive maximum at ~225 nm, although this was not systematically observed (Fig. 2). Thus, we focused on the specific absorption band at 225 nm since the absorption at ~205 nm may include the spectral signature of a statistical coil and would therefore be less representative of PPII. To confirm that the observed signal is indeed related to PPII, it was compared with ECD spectra recorded with increasing amounts of guanidine hydrochloride, GnCl, which is a specific PPII-inducer, like urea,[63] or with $CaCl_2$, which is a chaotropic (PPII destabilizing) agent.[26,27]

- PNRC-A: Despite biochemical evidence that the 285–295 region of PNRC associates with Grb2-SH3 domains,[15] no clear evidence of a positive band at λ ~225 nm was obvious for the peptide PNRC-A. Furthermore, $CaCl_2$ addition was accompanied by a 4,184 deg.dmol^{-1}.cm^2 decrease of the band at 225 nm, arguing some structuring events in the native PNRC-A. However, increasing amounts of GnCl (4.0 M, 6.0 M and 7.5 M) failed to induce an increase of the positive maximum at 225 nm, strongly suggesting that PNRC-A is poorly prone to adopt PPII (Figs. 2, 3a, 4). Not surprisingly, the behavior of PNRC-B (a PNRC2-derived sequence analogous to PNRC-A, where the aspartate in position 2 is replaced by a glutamate, i.e., residues 99 to 109, Table 1) is similar to that of PNRC-A (Figs. 2, 3b, 4).
- PNRC-C: The first four residues of the PNRC-C peptide correspond to the last four residues of PNRC-A and PNRC-B. Extended by the PPSHW pentapeptide (residues 296 to 300 in PNRC and 110 to 114 in PNRC2, Table 1), it encompasses a second PxxP motif that may interact with a domain of the ERα previously identified as an SH3-like domain.[18] The ECD spectrum of the nonapeptide Ac-VLPKPPSHW-NH_2 displayed a weak positive maximum at ~228 nm, which is most likely related to PPII content (Figs. 2, 3c, 4). This was confirmed by the fact that 4.0 M GnCl was sufficient to reach a positive maximum of absorbance ($\Delta[\theta]_{228}$ = 924 deg.dmol^{-1}.cm^2) while 6.0 M $CaCl_2$ was required to destabilize the conformation ($\Delta[\theta]_{228}$ = 1447 deg.dmol^{-1}.cm^2), as shown in Figures 3c and 4. Due to the positive band at 227 nm, it was possible to determine a percentage of PPII of ~ 53%.[25,29]
- PNRC-D: The PxxP-containing peptide PNRC-D (residues 38 to 44 of PNRC, Table 1), which corresponds to an N-terminal putative SH3-binding sequence only found in PNRC,[15] displays a weak positive maximum (positive band) at λ ~224 nm ([θ] = 716 deg. dmol^{-1}.cm^2), as shown in Figures 2, 3c, and 4. The intensity of this signal increases with increasing concentrations of GnCl (from $[\theta]_{224}$ = 613 deg.dmol^{-1}.cm^2 to $[\theta]_{224}$ = 2,171 deg.dmol^{-1}.cm^2), whereas 6 M of $CaCl_2$ were required for a modest decrease of the [θ] value. These absorbance behaviors might be attributed to a stronger and more stable PPII character than the above peptides.[43] Accordingly, it adopts ~ 61% PPII (Figs. 3d, 4).[25,29]

The evolution of the conformational state of PNRC-D in 6 M GnCl as a function of the temperature reveals that it is predominantly folded in PPII at low temperature (Fig. 5). The absence of any isodichroic point rules out a transition between two states but would be compatible with a redistribution of statistical populations in the favor of PPII.[49,53,55] Such a linear decrease of the PPII signature between 5 °C and 55 °C reflects a noncooperative character of the PPII structure, where each amino acid can explore different regions of the conformational space without influencing the other

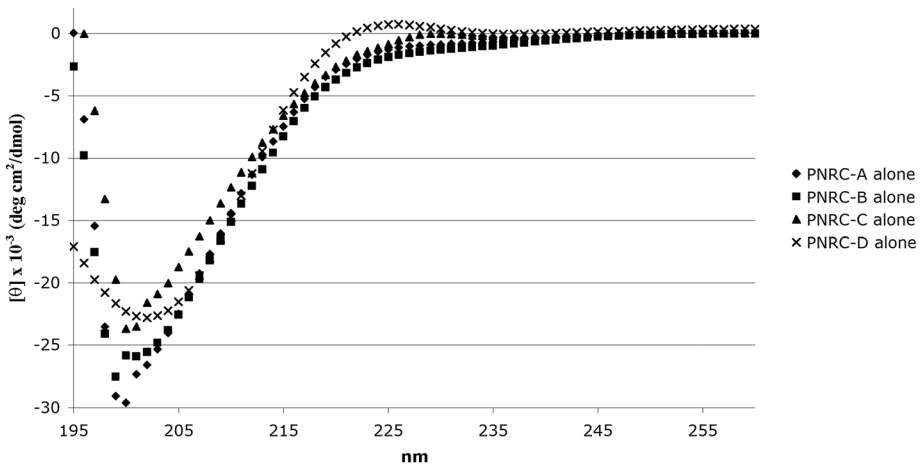

Fig. 2. ECD spectra between 195 nm and 260 nm of the peptides PNRC-A, PNRC-B, PNRC-C and PNRC-D recorded at 25 °C in water. The peptides were dissolved in a 10 mM phosphate-buffered solution (PNRC-A, B, C, and D at 30 μM). Absorbances are expressed in mean residue ellipticity ([θ], 10^{-3} deg. cm^2/dmol).

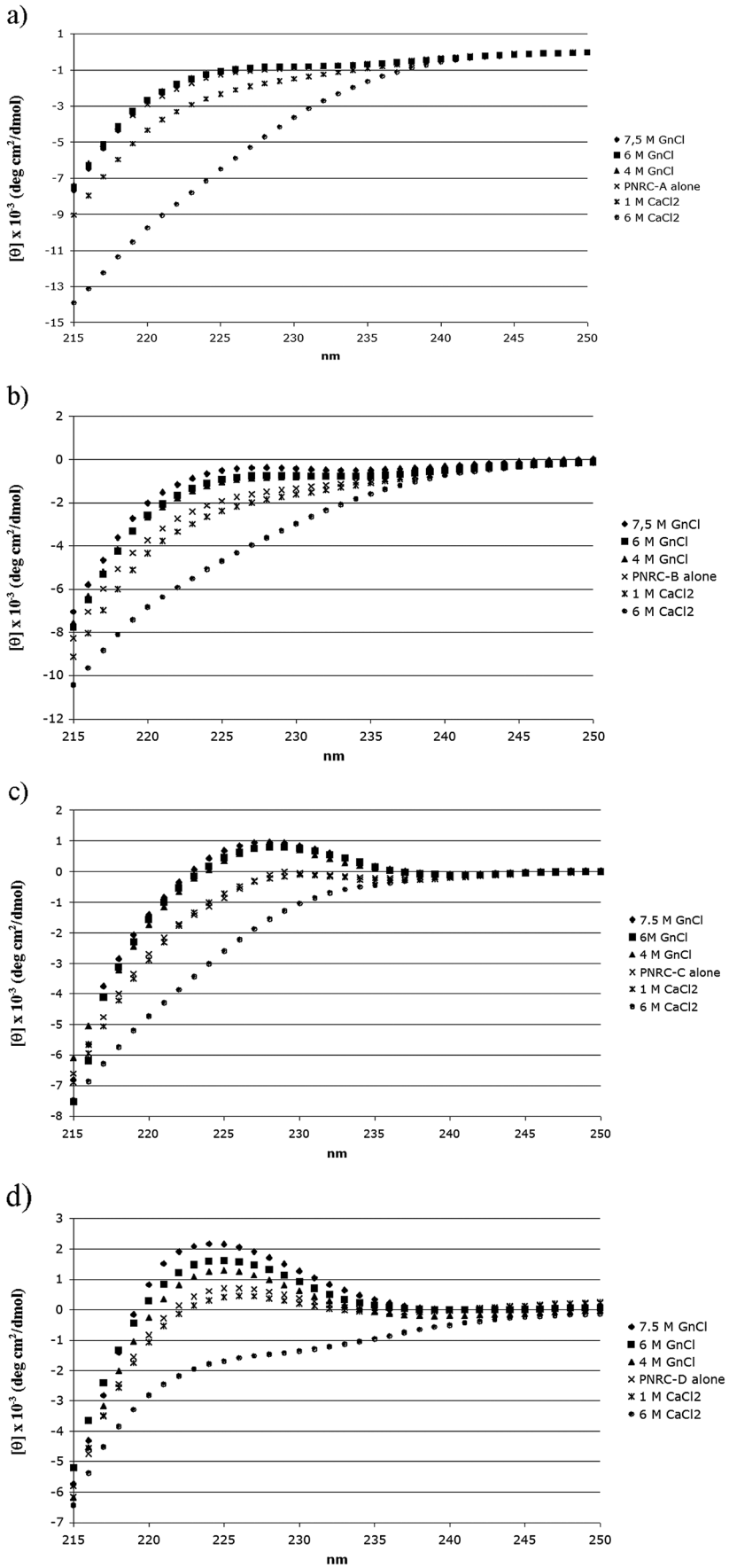

Fig. 3. ECD spectra recorded between 215 nm and 250 nm of the peptides (**a**) PNRC-A, (**b**) PNRC-B, (**c**) PNRC-C, and (**d**) PNRC-D. The spectra were recorded at 25 °C in phosphate and in the presence or absence of various concentrations of $CaCl_2$ (1 M or 6 M) or in GnCl (4.0 M, 6.0 M, 7.5 M). The peptides were dissolved in a 10 mM phosphate-buffered solution (PNRC-A, B, C, and D at 30 μM). Absorbances are expressed in mean residue ellipticity ([θ], 10^{-3} deg. cm^2/dmol).

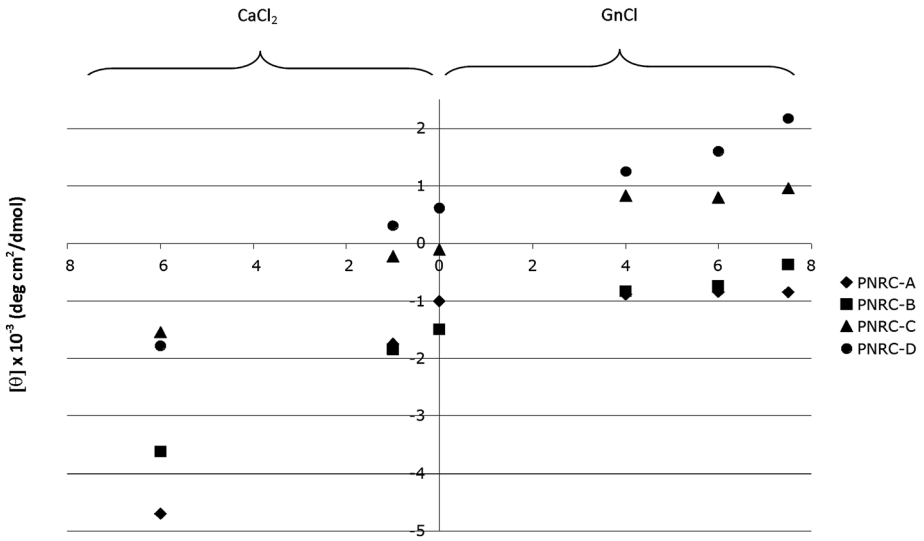

Fig. 4. GnCl (in M) and $CaCl_2$ (in M) dependency of the positive maxima in the ECD spectra ([θ], 10^{-3} deg. cm^2/dmol) for the peptides PNRC-A, PNRC-B, PNRC-C, PNRC-D.

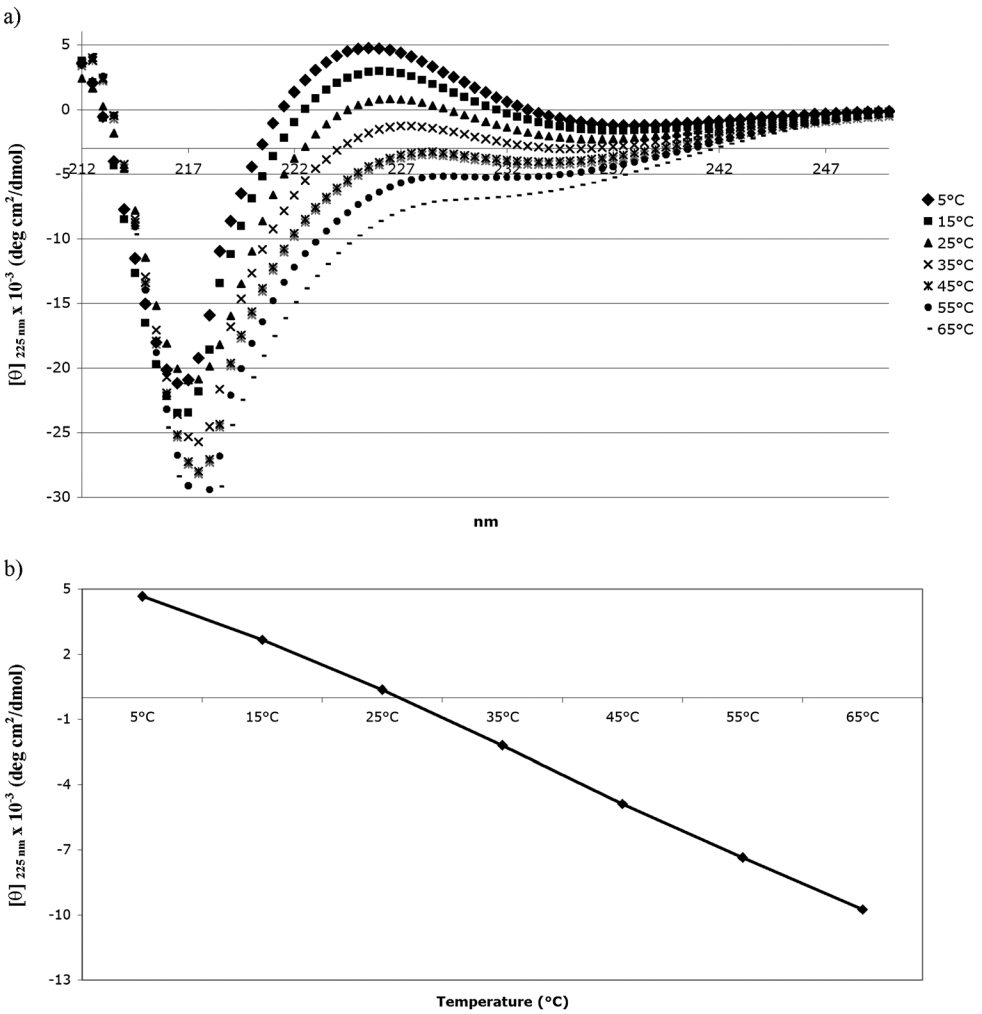

Fig. 5. (**a**) ECD spectra of the peptide PNRC-D as a function of the temperature. PNRC-D was dissolved in a 10 mM phosphate-buffered solution and diluted in a 6 M solution of GnCl. The spectra were recorded at 5 °C, 15 °C, 25 °C, 35 °C, 45 °C, 55 °C, and 65 °C in water. (**b**) Intensity of the circular dichroism recorded at 225 nm as a function of the temperature. Absorbances are expressed in mean residue ellipticity ([θ], 10^{-3} deg. cm^2/dmol).

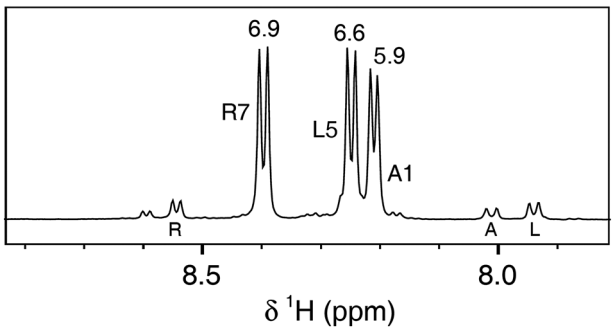

Fig. 6. Amide region of the ^{1}H-NMR spectrum of the PNRC-D peptide, H2O:D2O (90:10), pH 6.5, 295 K, 500 MHz. A1, L5 and R7 denote HN resonances of Ala-1, Leu-5, and Arg-7 in the major conformer, respectively. A, L, and R correspond to the HN chemical shifts in the minor conformer. The 3JHNHα coupling values (Hz) are displayed for the main resonances.

residues. This peculiar feature, related to locally driven PPII conformations in peptides, has been well described by several groups.[52,53,56,64,47,65–67]

Overall, PNRC-D, which has been claimed by Zhou et al. as the key SH3-binding motif of PNRC for Grb2,[15] displays the highest propensity to adopt PPII compared with the other peptides.

NMR spectroscopy. Based on the above findings, we embarked on a detailed structural analysis of the PNRC-D peptide by NMR spectroscopy. Each amide proton of the Ala, Leu, and Arg residues appeared as two doublets between 7.8 and 8.8 ppm, indicative of two slowly exchanging peptide conformations (Fig. 6). Some additional resonances were found at low temperature but accounted for as low as ~4% of the total population (Supporting Information, Fig. S1a). Integration of the two main doublets of Ala-1 gave 88% and 8% for a major and a minor conformer, respectively. The same population distributions were calculated for Leu-5 and Arg-7 residues.

2D rotating frame Overhauser effect (ROESY) spectroscopy revealed that the most abundant population was characterized by *trans* Xaa-Pro amide bonds (Xaa = Ala-1, Leu-5), as shown by the strong ROE correlations between the H^{α} of the residue Xaa and the two H^{δ} of the following proline. Moreover, the low chemical shift differences $^{13}C^{\beta}$ - $^{13}C^{\gamma}$ (ca. 4 ppm, Supporting Information, Table S2) confirmed a *trans* geometry for all Xaa-Pro moieties belonging to the main PNRC-D conformer.[68] Finally, chemical shift temperature coefficients $\Delta H^{N}/\Delta T$ of Ala-1, Leu-5 and Arg-7 were found to be very low (<-8 ppb/K), which is a strong indication that no hydrogen bonds were present (Supporting Information, Fig. S1b). Simulated annealing calculations were carried out using 26 interresidues distances and 19 dihedral restraints derived from 2D NMR experiments (Supporting Information, Tables S3–S5). Overlay of the best 10 structures obtained (Fig. 7) as well as the statistical analysis of the backbone angles (Supporting Information, Table 6) highlight that the major PNRC-D conformer corresponds to a canonical PPII structure, with ~60% PPII. However, a uniform φ-value of –170° was found for the Ala-1 residue and Arg-7 was associated with high RMSD value for φ, ψ, and χ_1 showing respectively a significant deviation or dynamics for both ends of the PPII chain. The side-chain of the central Leu-5 residue appears stabilized in a gauche (+) conformation, whereas the averaged values of $^{3}J_{H}\alpha_{H}\beta$ for Pro-2, Pro-3, and Pro-4 reflect a

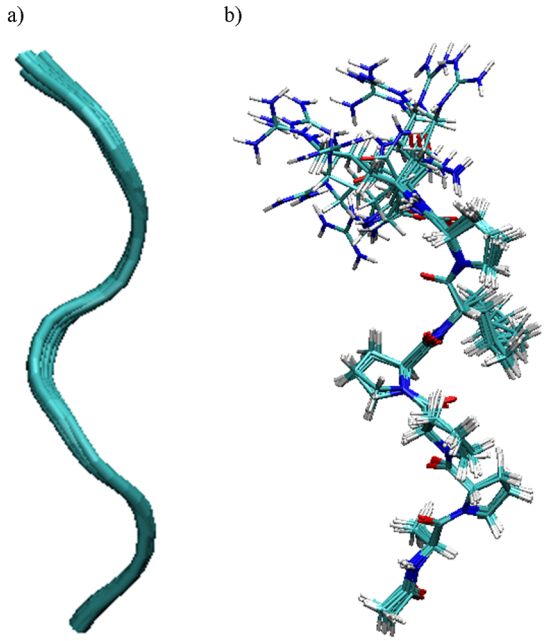

Fig. 7. Main PNRC-D conformation of the 10 best NMR structures. (**a**) backbone and (**b**) all atoms overlays, giving RMSD values of 0.35 Å and 0.68 Å for the region Ala-1 to Pro-6, respectively.

probable fast exchange between the up- and the down-puckering of the pyrrolidine rings (Supporting Information, Table S6).[69] Of note, these vicinal coupling constants would be also compatible with an envelope conformation. Pro-6 is distinguished in terms of ring puckering since calculations easily converged toward a defined χ_1 angle of -15° (*up* puckering). PPII stability was tested as a function of the temperature (Supporting Information, Fig. S1c). All $^{3}J_{H}N_{H}\alpha$ coupling constants were affected when increasing the sample temperature, including that of the central Leu-5 residue. This could be explained by a slight destabilization of the PPII conformation accompanied with more dynamics in the backbone chain, which is in good agreement with the ECD analysis.

Other PNRC-D conformers were also examined based on the minor amide proton resonances observed for Ala-1, Leu-5, and Arg-7. For Ala-1 and Leu-5, $^{3}J_{H}N_{H}\alpha$ values were found respectively 3.7 Hz and 2.7 Hz higher than previously, revealing local conformational changes of the backbone between the main and the minor conformations. More important, in the ROESY spectrum a cross-peak was detected between the Leu-5 H^{α} and the Pro-6 H^{α}, which characterizes a *cis* peptide bond.[26] Although such a cross-peak was not clearly identified between Ala-1 H^{α} and Pro-2 H^{α} due to severe spectral overlap, it seems very likely that the Ala-1–Pro-2 peptide bond is also experiencing the same *cis/trans* slow exchange process. Then, within the PNRC-D sequence, each non-Pro residue followed by a Pro (Ala-1 and Leu-5) is subjected to a *cis/trans* isomerization, where the *cis* population accounts for 8%. The minor resonance observed for the Arg-7 amide proton is probably due to the *cis/trans* isomerization of the preceding Leu-5–Pro-6 peptide bond. Indeed, strong spectral differences were found for amino acids directly experiencing *cis-trans* isomerization (Ala-1: $\Delta\delta$ = -0.20 ppm, $\Delta^{3}J_{H}N_{H}\alpha$ = +3.7 Hz; Leu-5: $\Delta\delta$ = -0.38 ppm, $\Delta^{3}J_{H}N_{H}\alpha$ = +2.7 Hz), whereas attenuated changes were observed for Arg-7 resonances ($\Delta\delta$ = 0.09 ppm, $\Delta^{3}J_{H}N_{H}\alpha$ = -0.1 Hz).

MD simulations. We were then interested in the stability of the NMR structures of the major conformer in solution at 300 K. Therefore, we undertook MD calculations using the generalized Born solvation model augmented with the hydrophobic solvent accessible surface area SA term. Trajectories of φ and ψ dihedral angles were analyzed for each PNRC-D amino acids during the time course of a 10 ns-long MD (Supporting Information, Fig. S7). Our results showed that Pro-2 and Pro-3 were only adopting the typical PPII dihedral angles (φ = -68 ± 8° and ψ = 153 ± 10° for Pro-2, φ = -67 ± 9° and ψ = 154 ± 10° for Pro-3), whereas Pro-6 displayed 85 % PPII (φ = -64 ± 9° and ψ = 143 ± 12°) and a weak propensity (15% of the dynamics time) to populate the α-helical region of the Ramachandran plot (φ = –71 ± 9° and ψ = –20 ± 18°). This behavior was even more pronounced for Pro-4, which showed a slight preference for the α-helix dihedral angles (59% of the time course, φ = -75 ± 9° and ψ = -11 ± 15°) in exchange with the regular PPII (φ = -70 ± 9° and ψ = 147 ± 15°), as shown in Figure 8. Ala-1 and Leu-5 also displayed two fast exchanging conformational states, the first being the PPII extended structure and the second a β-sheet-like conformation. However, both amino acids preferred the PPII (60 % of the time course for Ala-1 and 63 % of the time course for Leu-5). For Ala-1, the dihedral angle values were φ = -78 ± 12° and ψ = 148 ± 10° for the PPII conformation, and φ = –138 ± 12° and ψ = 150 ± 11° for the β-sheet conformation. For Leu-5, the dihedral angle values were φ = –77 ± 13° and ψ = 147 ± 12° for the PPII conformation, and φ = –134 ± 11° and ψ = 136 ± 20° for the β-sheet conformation. Finally, as observed in the NMR structures,

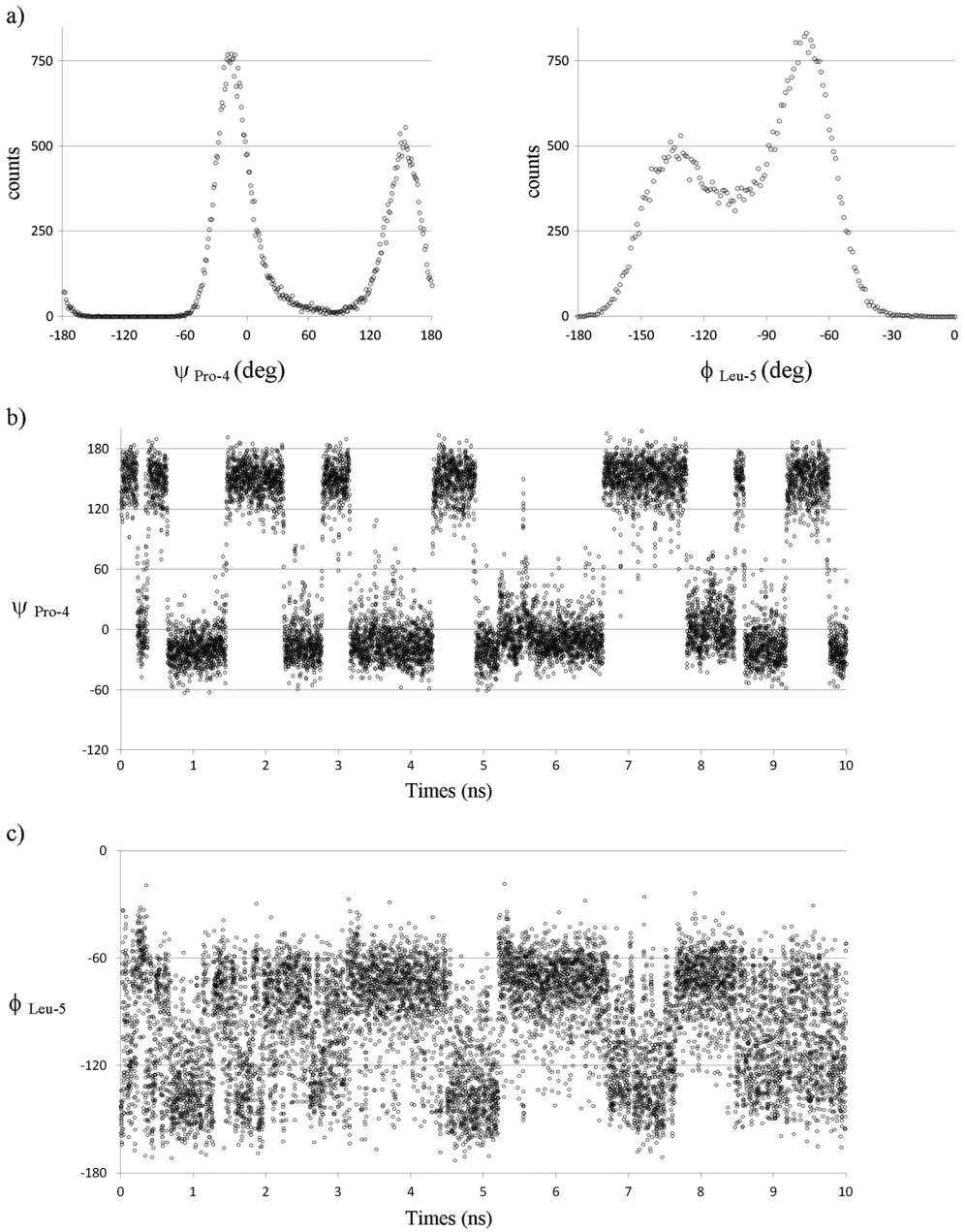

Fig. 8. MD results obtained on the Pro-4–Leu-5 segment. (**a**) Populations observed for ψPro-4 and ϕLeu-5 during a 10 ns MD simulation. 50,000 structures were extracted from the dynamics for the statistical analysis. Trajectories obtained for (**b**) ψPro-4 and (**c**) ϕLeu-5 during the 10 ns MD simulation.

Arg-7 displayed a much more flexible behavior, exchanging between α-helical (ca. 30% of the MD time course), β-sheet (ca. 40%), and the PPII (ca. 30%) conformations.

Although the high stability of the PPII conformation found by NMR was confirmed for most of the PNRC-D residues, the dynamics carried out at 300 K provided additional information. A first observation is the occurrence of breaks in the PPII structure as a consequence of the PPII α-helix conversion of Pro-4. This constitutes the main deviation from the ideal PPII structure for PNRC-D, the Ala-1−Pro-4 and Pro-4−Pro-6 segments being most of the time well stabilized in this extended conformation. The comparison of the φ- and ψ-trajectories recorded for each amino acid revealed that no clear correlation exists between the conformational transitions. This provides direct evidence that the PPII structure is not cooperative, each amino acid behaving independently.[47,52,53] However, most of the time the conformational jump observed for the Pro-4 ψ-dihedral angle was accompanied with a φ- rearrangement of the following Leu-5 (Fig. 8).

Biochemistry

Interaction with Grb2. Grb2 is a small adaptor protein of 217 amino-acids (25 kDa) containing two SH3 domains (SH3–SH2–SH3) that associate with PPII motifs sharing a PxxP signature. Because of the ability of Grb2 to recruit PNRC, we measured the dissociation constant of the PNRC-D/Grb2 complex by using fluorescence spectroscopy,[70] each SH3 domain encompassing a tryptophan residue appropriate for quenching fluorescence under ligand association (Trp-36 for the N-terminal Grb2 SH3 domain[71] and Trp-194 for the C-terminal Grb2 SH3 domain[72]). The Grb2 peptide ligand V10R (VPPPVPPRRR), which is issued from the Grb2 agonist protein Son-of-Sevenless (Sos),[73–75] was used as a reference. As expected, V10R, which is highly structured in PPII in solution,[26] interacts with Grb2 SH3 domains (Kd = 3.67 μM). However, a weak affinity was observed for the most PPII-structured peptide PNRC-D (Kd > 300 μM, Fig. 9).

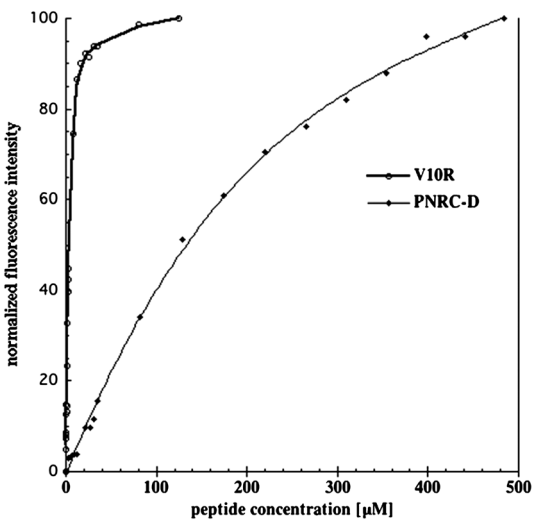

Fig. 9. Fluorescence change of Grb2 (1 μM in 50 mM Tris buffer adjusted to pH 8.0) by V10R and the peptide PNRC-D upon the addition of 5 μL of each at 10-3 M or 10-4 M in Tris buffer. Experiments conducted at 18 °C. Excitation and emission wavelengths were λ = 280 nm and λ = 350 nm, respectively. Experimental datapoints have been fitted with the Monte-Carlo based MC-Fit program.[36]

Thus, we attempted to increase the binding affinity of PNRC-D for Grb2 by exploring the effects of different peptide derivatives (longer peptides or dimers) appropriate for an efficient fitting on both Grb2-SH3 domains.[74–76]

At first, we tested the entire C-terminal proline-rich region of PNRC (i.e., PNRC-E, residues 285 to 300) and PNRC2 (i.e., PNRC-G, residues 99 to 114), which encompasses two successive PxxP SH3-binding motifs. It is of note that fluorescence spectroscopy binding assays were also performed in the absence of the C-terminal tryptophan (PNRC-F), to discount possible fluorescence interference. As no fluorescence changes were observed, we concluded that this tryptophan did not interfere. PNRC-G failed to interact with Grb2.

Vidal et al.[76] have defined the lysine side-chain as a highly appropriate linker for spanning both Grb2 SH3 domains, allowing an increase in affinity of two to three orders of magnitude (from Kd = 18±1.1 μM for the V10R monomer to Kd = 0.04±0.005 μM for the V10R dimer).[74–76] Thus, we tested the two lysine-linked heterodimers PNRC-H and PNRC-I (Table 1), which combine the two N- and C-terminal SH3 binding proline-rich sequences of PNRC (both have been proposed to be necessary for Grb2 recognition[15]). Since the spatial orientation (i.e., class I or class II orientation[73]) of the 38-44 PNRC sequence is unknown with respect to its 285–295 counterpart, we tested the affinity for Grb2 of PNRC-H (38 to 44, 291 to 285) and PNRC-I (38 to 44, 285 to 291). Neither PNRC-H nor PNRC-I interacted with Grb2, while it was claimed that these two regions are cooperative with respect to Grb2 binding.[15]

Although a rational peptide design (i.e., proline-rich peptide containing a PxxP signature, structured in PPII and sharing a conserved basic residue important for the stabilization of the peptide / SH3 complex), no interaction with Grb2 SH3 domain was detected. These results suggest the presence of yet unidentified regions important for PNRC/Grb2 interaction and different from the solely PxxP motifs. Likewise, a mode of binding of proline-rich regions issued from Grb2 antagonists (PNRC and PNRC2) could be different from those derived from Grb2 agonists such as Sos.

Interaction with ERα. In our ELISA-based competitive test (Fig. 1b), PNRC-A and PNRC-B, both of which are poorly structured in PPII, decrease by ~20% the interaction of ERα with ERα17p adsorbed to a matrix at 1 and 10 μM (Fig. 1c). Although the specificity of this inhibition observed at such a high concentration may be subject to controversy, it should be noted that PNRC-C and PNRC-D, which share higher PPII character, decreased the interaction by ~40% at 10 μM (Fig. 1c). Hence, these PxxP-containing peptides issued from PNRC and PNRC2 appear to interact in the P295-T311 region of ERα in charge of the recruitment of various proteins modulating its conformation and activity,[19–23] in a PPII-dependent manner. In this context, it should be stressed that the presence or absence of estradiol at 1 μM or the strong antiestrogen fulvestrant at 10 μM did not modify these results (data not shown). Thus, these peptides (PNRC fragments) would act in a ligand-independent manner, contrasting with the observations made with whole PNRC and PNRC2.[16]

DISCUSSION

PNRC and PNRC2 are nuclear receptor coactivators operating after translocation of the receptor into the nucleus.[15,77] PNRC interferes with different nuclear proteins such as nuclear hormone receptors including ERα[16] and the

polymerase III subunit RPC39.[78] In addition, it interacts with Grb2 SH3 domains, resulting in an inhibition of the Grb2/Sos/Ras/raf/MEK/ERK cascade as well as its activation potency of ERα activity.[15]

In the present work, we synthesized a number of peptides derived from PNRC and PNRC2 and containing the structural requirements for an efficient association with Grb2 SH3 domains, i.e., PxxP motifs, PPII secondary structure, and the presence of H-bond donor residues (lysine, arginine).[38–42] ECD experiments revealed that the synthetic peptides adopt PPII in the following decreasing order: PNRC-D > PNRC-C > PNRC-A PNRC-B (Figs. 3, 4).

The sequence corresponding to PNRC-D (residues 38 to 44 of PNRC) and found in the N-terminus of PNRC only, displayed the highest amount of PPII (Figs. 3, 4). This propensity was supported by the ECD spectra recorded as a function of the temperature (Fig. 5) and in the presence or absence of GnCl and $CaCl_2$ (Figs. 3d, 4). Likewise, it was supported by 2D NMR-restrained simulated annealing (Figs. 6, 7) and MD calculations (Fig. 8). However, it is noteworthy that most of our peptides contain a PS motif, which has been reported to be associated with type II β-turns.[79] Even if we cannot totally exclude a contribution of type II β-turn, some arguments are in favor of a predominant PPII form: (i) the spectra are poorly relevant to typical type II β-turn[80,81]; (ii) PS-related type II β-turn is principally observed in high concentrations of TFE, a hydrogen-bond promoting agent not used here,[82]; (iii) the effects induced by the chaotropic agent GnCl are known to be closely related to PPII-like conformations; (iv) the intensity of the negative maximum at ~200 nm for our PNRC peptides is higher than the one recorded at ~225 nm, a feature specific to the PPII CD signature; (v) the CD study of the peptide PNRC-D in function of the increase of the temperature shows an increase of the intensity of the signal at ~224 nm and a decrease of the intensity of the signal at ~210 nm, a process that is also relevant to PPII; (vi) the PS motifs are comprised for most of the reported peptides in a PxxP consensus sequence, which is known to bind PPII cognate domains such as SH3 and WW; and (vii) our NMR/computational combined approach favors PPII. Overall, we assume that a type II β-turn is not predominant for the PNRC peptides. In this regard, recent theoretical studies have shown that PS motifs can be found in PPII.[83]

The Grb2 protein partner PNRC, which comprises N- (residues 38 to 44) and C- (residues 285 to 311) terminal proline-rich (PxxP) SH3-binding sequences, interacts with Grb2 SH3 domains,[15] in contrast to PNRC2, which contains only the C-terminal proline-rich regions of PNRC.[15] Thus, the N-terminal counterpart appears crucial for such an interaction. Accordingly, we observed that the peptide PNRC-D (residues 38 to 44 of PNRC), which corresponds to the N-terminal PxxP sequence of PNRC, exhibits the highest content of PPII and interacts, though weakly, with Grb2 (Kd > 300 μM, Fig. 9).

This particularly low affinity suggests the involvement of other regions of PNRC such as a second PxxP motif fitting to the second Grb2 SH3 domain. Thus, we synthesized and tested peptide dimers in which each monomer contains a PxxP motif issued from PNRC. Among the three putative SH3-binding regions present in PNRC (i.e., A^{38}PPPLPR,[44] S^{285}DPPSPS^{291}, and V^{292}LPKPPSHW^{300}, Scheme 1 and Table 1), the 38–44 and 285–291 regions have been reported as essential for Grb2 interaction,[15] an observation that reinforces the involvement of PPII. Taking into account the two putative orientations (type I or type II orientations) for PPII SH3 binding peptides and the optimal distance between monomers for an efficient interaction with the two Grb2 SH3 domains,[72,84] we tested the branched peptide dimers PNRC-G (Ac-APPPLPRK(AcSPSPPDS)-NH_2) and PNRC-H (Ac-APPPLPRK(AcSDPPSPS)-NH_2). Unfortunately, these two peptide dimers failed to interact with Grb2. Next, the sequences encompassing the two successive C-terminal PxxP motifs, i.e., PNRC-E (Ac-SDPPSPSVLPKPPSHW-NH_2) and PNRC-G (Ac-SEPPSPSVLPKPPSHW-NH_2), were assayed, but again, no interaction was detected, confirming the importance of the N-terminal proline-rich region.[15] Hence, interaction between PNRC and Grb2 differs from other reported Grb2 complexes and could require a more sophisticated signal than the existence of the solely PxxP signature. Despite the presence of PPII and positive charges (both important for SH3 association), only PNRC-D interacted, although weakly, with Grb2, contrasting with previously published biochemical studies.[15] The weak interaction (hydrophobic in nature), out of the context of the entire protein, can be supported by several hypotheses:

- The lack of control of various thermodynamic parameters related to ligand-binding or to the stabilization of prenative states required for ligand association (control of the entropy-driven elasticity of the peptide,[43] of proline ring puckering, of *cis/trans* isomerization, etc.), although proline has a restricted flexibility (i.e., low entropy at the residue level) due to its pyrrolidine ring. Indeed, proline residues from PPII are crucial for SH3 domain association (confirming the importance of hydrophobic contacts[85]) in addition to a hydrogen bond implying a basic residue at the N-terminus (class I ligand) or the C-terminus (class II ligand).[85,39,86,87]
- The length of the peptide (or a number of prolines) is not sufficient for efficient protein–peptide recognition, potentially through additional binding sites. Due to the limited binding surface of SH3 domains and their high flexibility, PPII binds rapidly and reversibly with modest affinities that are usually in the micromolar range, suggesting that other fragments are required.[39,86] In this context, a PPII peptide issued from biased phage display libraries, presenting similarities with PNRC-D and flanked in C-terminus by five residues (APPLPPRNRPRL) has been shown to occupy a large surface between the RT and the n-Src loops of the Src SH3 domain. Accordingly, the sequence APPLPPRNPRL exhibits a 20-fold increased affinity for the Src-SH3 domain compared to the APPLPPR sequence.[88]
- In a physiological context, one must evoke a possible role of the phosphorylation at the serine residue preceding the proline and present in most of the synthesized peptides. Indeed, PxSP motifs (where x corresponds to any amino-acid), which are commonly recognized by the MAP2 or $p34^{cdc2}$ kinases, are responsible for ligand binding and related regulation.[40] This may explain the discrepancy between our results and those published by Zhou et al.[15]
- Since Sos is a Grb2 agonist,[89] while PNRC is an antagonist,[15] a mode of binding PNRC different from the Sos sequence (V10R, VPPPVPPRRR) is not excluded.

Hence, the reasons for which V10R, which is structured in PPII and shares a PxxP signature, interacts efficiently with Grb2 (Kd = 67 μM), while PNRC-D, which encompasses the same required structural features with respect to SH3 binding and interacts only weakly with Grb2 (Kd > 300 μM, Fig. 9), should be further studied.

Remarkably and independently from the presence of a C-terminal LxxLL motif, PNRC and PNRC2 interact with ERα through their C-terminus SH3-binding motifs, i.e., SDPPSPS (residues 286 to 291 of PNRC, Scheme 1) and SEPPSPS (residues 98 to 108 of PNRC2, Scheme 1), inducing thereby ERα-dependent transcription.[16] These observations suppose that ERα encompasses at its surface an SH3-like domain appropriate for PxxP recognition. In connection with these statements and with respect to ERα interaction, PNRC-A, -B, -C, and –D were found to compete with ERα17p.

We proposed in a previous theoretical-based study that the AF-2 subregion flanking the type II β-turn (residues 364 to 367 of ERα) and the one turn helix H4 (residues 367 to 370 of ERα) of ERα could participate in PPII association.[18] Strikingly, Zhou et al.[16] demonstrated through mutagenesis that the residues Ile-358, Lys-362, and, to a lesser extent, Val-376 are important for the recognition of the SH3-binding motifs of PNRC. The type II β-turn and the helix H4 being overlapped by a motif of the hinge region with which it may interact, i.e., PLMIKRSKKNSLALSLT (ERα17p: residues 295-311, Fig. 1a), we tested the ability of PNRC-A, -B, -C, and –D to interfere with this interaction (Fig. 1b). These peptides were able to compete with the binding of ERα to surface-bound ERα17p (especially PNRC-C and -D) as did ERα17p itself (Inset, Fig. 1c). It should be stressed that no binding difference was recorded in the presence of estradiol or fulvestrant, indicating that the association of PxxP motifs of these PNRC fragments with the ERα AF2 region of the receptor is ligand-independent, contrasting with the data reported by Zhou et al. for the full-length protein.[16] In this context, using an ELISA approach (Active Motif NR assay[19,90]), we evaluated the possibility of interactions of our peptides with the LxxLL-binding groove of ERα, the expression of which is under the control of estrogenic/antiestrogenic ligands. No interaction was detected, confirming our view of the independence of binding between these PNRC fragments and agonistic or antagonistic ERα ligands.

CONCLUSION

In the present work, we show that peptides encompassing a PxxP signature derived from the proline-rich regions of PNRC and PNRC2 are, to varying degrees, structured in PPII. This constitutes the first structural study with respect to these coactivators. We also provide evidence that the more they exhibit a PPII signature, the more they interact with a region of the ERα located in the close vicinity of the type II β-turn / H4 region previously reported by our group as a potential PPII-binding region.[18] To our knowledge, this is the first description of an intermolecular PPII/ERα interaction. Hence, the present study validates our view based on a theoretical approach[18] opening new avenues for the control of ERα-related transcription. However, and somewhat surprisingly, peptides containing the PxxP signature failed to bind efficiently with Grb2-SH3 domains, suggesting more complex molecular mechanisms than those described for agonists such as Sos. Gratifyingly, our observations confirm the results of Zhou et al.[16] and present convincing evidence that short PPII peptides bind to liganded or unliganded ERα and may be responsible for some of the biological actions observed in ERα-positive cells and tumors in the absence of the cognate ligand.

ACKNOWLEDGMENTS

We thank T. Blasco, G. Clotide and Dr. Gerard Bolbach (UMR 7203, Université Pierre et Marie Curie, Ecole Normale Supérieure, Paris) for mass spectrometry experiments. We also thank Elodie Cosnefroy (Paris) for active participation in peptide synthesis and circular dichroism studies as well as to Jonathan Goffinet and Pierre-Alain Lecuyer (Institut Meurice, Brussels) for ELISA development. We thank the Natural Substances Laboratory of Meurice Institute for the gift of the biotinylated ERα17p. The authors received financial support from the Centre National pour la Recherche Scientifique (CNRS), the MEDIC Fundation and the Belgian Fund for Medical Scientific Research (Grant no. 3.4512.03), and the "Fonds J.-C. Heuson de Recherche en Cancérologie Mammaire."

LITERATURE CITED

1. Clemons M, Danson S, Howell A. Tamoxifen ("Nolvadex"): a review. Cancer Treat Rev 2002;28:165–180.
2. Scott SM, Brown M, Come SE. Emerging data on the efficacy and safety of fulvestrant, a unique antiestrogen therapy for advanced breast cancer. Expert Opin Drug Saf 2011;10:819–826.
3. Hall JM, Chang CY, Mc Donnell DP. Development of peptide antagonists that target estrogen receptor β-coactivator interactions. Mol Endocrinol 2000;14:2010–2023.
4. Rodriguez AL, Tamrazi A, Collins ML, Katzenellenbogen JA. Design, synthesis, and in vitro biological evaluation of small molecule inhibitors of estrogen receptor α coactivator binding. J Med Chem 2004;47:600–611.
5. Leclercq G, Gallo D, Cossy J, Laïos I, Larismont D, Laurent G, Jacquot Y. Peptides targeting estrogen receptor alpha —potential applications for breast cancer treatment. Curr Pharm Design 2011;17:2632–2653.
6. Horwitz KB, Jackson TA, Bain DL, Richer JK, Takimoto GS, Tung L. Nuclear receptor coactivators and corepressors. Mol Endocrinol 1996;10:1167–1177.
7. Katzenellenbogen JA, O'Malley BW, Katzenellenbogen BS. Tripartite steroid hormone receptor pharmacology: interaction with multiple effector sites as a basis for the cell- and promoter-specific action of these hormones. Mol Endocrinol 1996;10:119–131.
8. Glass CK, Rose DW, Rosenfeld MG. Nuclear receptor coactivators. Curr Opin Cell Biol 1997;9:222–232.
9. McInerney EM, Rose DW, Flynn SE, Westin S, Mullen TM, Krones A, Inostroza J, Torchia J, Nolte RT, Assa-Munt N, Milburn MV, Glass CK, Rosenfeld MG. Determinants of coactivator LXXLL motif specificity in nuclear receptor transcriptional activation. Genes Dev 1998;12:3357–3368.
10. McKenna NJ, Xu J, Nawaz Z, Tsai SY, Tsai MJ, O'Malley BW. Nuclear receptor coactivators: multiple enzymes, multiple complexes, multiple functions. J Steroid Biochem Mol Biol 1999;69:3–12.
11. Pike ACW, Brzozowski AM, Hubbard RE. A structural biologist's view of the oestrogen receptor. J Steroid Biochem Mol Biol 2000;74:261–268.
12. Savkur RS, Burris TP. The coactivator LXXLL nuclear receptor recognition motif. J Pept Res 2004;63:207–212.
13. Lonard DM, O'Malley BW. Expanding functional diversity of the coactivators. Trends Biochem Sci 2005;30:126–132.
14. Zhou D, Quach KM, Yang C, Lee SY, Pohajdak B, Chen S. Receptor coregulatory protein that modulates transcriptional activation of multiple nuclear receptors including orphan receptors SF1 (Steroidogeic Factor 1) and ERRα1 (Estrogen Related Receptor α-1). Mol Endocrinol 2000;14:986–998.
15. Zhou D, Chen B, Ye JJ, Chen S. A novel crosstalk mechanism between nuclear receptor-mediated and growth factor/Ras-mediated pathways through PNRC-Grb2 interaction. Oncogene 2004;23:5394–5404.
16. Zhou D, Ye JJ, Li Y, Lui K, Chen S. The molecular basis of the interaction between the proline-rich SH3-binding motif of PNRC and estrogen receptor alpha. Nucl Acids Res 2006;34:5974–5986.

17. Zhou D, Chen S. PNRC2 is a 16 kDa coactivator that interacts with nuclear receptors through an SH3-binding motif. Nucl Acids Res 2001;29:3939–3948.
18. Jacquot Y, Gallo D, Leclercq G. Estrogen receptor alpha — identification by a modelling approach of a potential polyproline II recognizing domain within the AF-2 region of the receptor that would play a role of prime importance in its mechanism of action. J Steroid Biochem Mol Biol 2007;104:1–10.
19. Gallo D, Jacquot Y, Cleeren A, Jacquemotte F, Laios I, Laurent G, Leclercq G. Molecular basis of agonistic activity of ERα17p, a synthetic peptide corresponding to a sequence located at the N-terminal part of the estrogen receptor α ligand binding domain. Lett Drug Design Discov 2007;4:346–355.
20. Gallo D, Leclercq G, Jacquot Y. The N-terminal part of the ligand-binding domain of the human estrogen receptor α: a new target for estrogen disruptors. In: Colombo GP, Ricci S, editors. Medicinal chemistry research progress. New York: Nova, NY; 2009. p 207–224.
21. Carlier L, Byrne C, Miclet E, Bourgoin-Voillard S, Nicaise M, Tabet JC, Desmadril M, Leclercq G, Lequin O, Jacquot Y. Biophysical studies of the interaction between calmodulin and the R287-T311 region of human estrogen receptor a reveals an atypical binding process. Biochem Biophys Res Commun 2012;419:356–361.
22. Gallo D, Haddad I, Duvillier H, Jacquemotte F, Laios I, Laurent G, Jacquot Y, Vinh J, Leclercq G. Trophic effect in MCF-7 cells of ERα17p, a peptide corresponding to a platform regulatory motif of the estrogen receptor α — underlying mechanisms. J Steroid Biochem Mol Biol 2008;109:138–149.
23. Gallo D, Jacquot Y, Laurent G, Leclercq G. Calmodulin, a regulatory partner of the estrogen receptor alpha in breast cancer cells. Mol Cell Endocrinol 2008;291:20–26.
24. Dalcol I, Pons M, Ludevid MD, Giralt E. Convergent synthesis of repeating peptides (Val-X-Leu-Pro-Pro-Pro)8 adopting a polyproline II conformation. J Org Chem 1996;61:6775–6782.
25. Kelly MA, Chellgren BW, Rucker AL, Troutman JM, Fried MG, Miller AF, Creamer TP. Host-guest study of left-handed polyproline II helix formation. Biochemistry 2001;40:14376–14383.
26. Miclet E, Jacquot Y, Goasdoue N, Lavielle S. Solution structural study of a proline-rich decapeptide. C R Chim 2008;11:486–492.
27. Kapitán J, Gallo D, Goasdoué N, Nicaise M, Desmadril M, Hecht L, Leclercq G, Barron LD, Jacquot Y. Identification of a human estrogen receptor α-derived antiestrogenic peptide that adopts a polyproline II conformation. J Pept Sci 2009;15:455–464.
28. Rucker AL, Pager CT, Campbell MN, Qualls JE, Creamer TP. Host-guest scale of left-handed polyproline II helix formation. Proteins Struct Funct Bioinform 2003;53:68–75.
29. Parot I, Huang PC, Khosla C. Circular dichroism and nuclear magnetic resonance spectroscopic analysis of immunogenic gluten peptides and their analogs. J Biol Chem 2002;277:45572–45578.
30. Keller RLJ. The computer aided resonance assignment tutorial, Ed. Goldau, Switzerland: Cantina Verlag; 2004.
31. Delaglio F, Grzesiek S, Vuister GW, Zhu G, Pfeifer J, Bax A. NMRPipe: a multidimensional spectral processing system based on UNIX pipes. J Biomol NMR 1995;6:277–293.
32. Shen Y, Delaglio F, Cornilescu G, Bax A. TALOS plus: a hybrid method for predicting protein torsion angles from NMR chemical shifts. J Biomol NMR 2009;44:213–223.
33. Case DA, Cheatham T, Darden T, Gohlke H, Luo R, Merz KM, Onufriev A, Simmerling C, Wang B, Woods RJ. The Amber biomolecular simulation programs. J Comput Chem 2005;26:1668–1688.
34. Case DA, Darden TA, Cheatham TE, Simmerling CL, Wang J, Duke RE, Luo R, Walker RC, Zhang W, Merz KM, Roberts B, Wang B, Hayik S, Roitberg A, Seabra G, Kolossváry I, Wong KF, Paesani F, Vanicek J, Liu J, Wu X, Brozell SR, Steinbrecher T, Gohlke H, Cai Q, Ye X, Wang J, Hsieh MJ, Cui G, Roe DR, Mathews DH, Seetin MG, Sagui C, Babin V, Luchko T, Gusarov S, Kovalenko A, Kollman PA. 2010, AMBER 11, University of California, San Francisco.
35. Guilloteau JP, Fromage N, Rieskautt M, Reboul S, Bocquet D, Dubois H, Faucher D, Colonna C, Ducruix A, Becquart J. Purification, stabilization, and crystallization of a modular protein: Grb2. Protein Struct Funct Genet 1996;25:112–119.
36. Dardel F. MC-Fit: using Monte-Carlo methods to get accurate confidence limits on enzyme parameters. Comput Appl Biosci 1994;10:273–275.
37. Corpet F. Multiple sequence alignment with hierarchical clustering. Nucleic Acids Res 1988;16:10881–10890.
38. Aitio O, Hellman M, Kazlauskas A, Vingadassalom DF, Leong JM, Saksela K, Permi P. Recognition of tandem PxxP motifs as a unique Src homology 3-binding mode triggers pathogen-driven actin assembly. Proc Natl Acad Sci U S A 2010;107:21743–21748.
39. Williamson MP. The structure and function of proline-rich regions in proteins. Biochem J 1994;297:249–260.
40. Kay BK, Williamson MP, Sudol M. The importance of being proline: the interaction proline-rich motifs in signaling proteins with their cognate domain. FASEB J 2000;14:231–241.
41. Rath A, Davidson AR, Deber CM. The structure of "unstructured" regions in peptides and proteins: role of the polyproline II helix in protein folding and recognition. Biopolymers 2005;80:179–185.
42. Cubellis MV, Caillez F, Blundell TL, Lovell SC. Properties of polyproline II, a secondary structure element implicated in protein-protein interactions. Proteins 2005;58:880–892.
43. Tiffany ML, Krimm S. New chain conformation of poly(glutamic acid) and polylysine. Biopolymers 1968; 6: 1379–1382.
44. Rucker AL, Creamer TP. Polyproline II helical structure in protein unfolded states: lysine peptides revisited. Protein Sci 2002;11:980–985.
45. Ferreon JC, Hilser VJ. The effect of polyproline II (PPII) conformation on the denaturated state entropy. Protein Sci 2003;12:447–457.
46. Shi Z, Olson CA, Rose GD, Baldwin RL, Kallenbach NR. Polyproline II structure in a sequence of seven alanine residues. Proc Natl Acad Sci U S A 2002;99:9190–9195.
47. Chen K, Liu Z, Kallenbach NR. The polyproline II conformation in short alanine peptides is noncooperative. Proc Natl Acad Sci U S A 2004;101:15352–15357.
48. Chen K, Liu Z, Zhou C, Shi Z, Kallenbach NR. Neighbor effect on PPII conformation in alanine peptides. J Am Chem Soc 2005;127:10146–10147.
49. Bochicchio B, Tamburro AM. Polyproline II structure in proteins: identification by chiroptical spectroscopies, stability and functions. Chirality 2002;14:782–792.
50. Bochicchio B, Pepe A, Tamburro AM. Investigating by CD the molecular mechanism of elasticity of elastomeric proteins. Chirality 2008;20:985–994.
51. Stapley BJ, Creamer TP. A survey of left-handed polyproline II helices. Protein Sci 1999;8:587–595.
52. Creamer TP. Left-handed polyproline II helix formation is (very) locally driven. Proteins 1998;33:218–226.
53. Gokce I, Woody RW, Anderluh G, Lakey JH. Single peptide bonds exhibit poly(Pro)II ("random coil") circular dichroism spectra. J Am Chem Soc 2005;127:9700–9701.
54. Kuemin M, Schweitzer S, Ochsenfeld C, Wennemers H. Effects of terminal functional groups on the stability of polyproline II structure: a combined experimental and theoretical study. J Am Chem Soc 2009;131:15474–15482.
55. Park SH, Shalongo W, Stellwagen E. The role of PPII conformations in the calculation of peptide fractional helix content. Protein Sci 1997; 6:1694–1700.
56. Schweitzer-Steiner R, Eker F, Griebenow K, Cao X, Nafie LA. The conformation of tetraalanine in water determined by polarized raman, FT-IR, and VCD spectroscopy. J Am Chem Soc 2004;126:2768–2776.
57. Asher SA, Mikhonin AV, Bykov S. UV raman demonstrates that α-helical polyalanine peptides melt polyproline II conformations. J Am Chem Soc 2004;126:8433–8440.
58. Schweitzer-Stenner R, Measey T, Kakalis L, Jordan F, Pizzanelli S, Forte C, Griebenow K. Conformations of alanine-based peptides in water probed by FTIR, raman, electronic circular dichroism, an NMR spectroscopy. Biochemistry 2007;46:1587–1596.
59. Schweitzer-Steiner R, Measey TJ. The alanine-rich XAO peptide adopts a heterogenous population, including turn-like and polyproline II conformations. Proc Natl Acad Sci U S A 2007;194:6649–6654.
60. Graf J, Nguyen PH, Gerhard S, Schwalbe H. Structure and dynamics of the homologous series of alanine peptides: a joint molecular dynamics/ NMR study. J Am Chem Soc 2007;129:1179–1189.
61. Oh KI, Lee KK, Park EK, Yoo DG, Hwang GS, Cho M. Circular dichroism eigenspectra of polyproline II and β-strand conformers of trialanine in water: singular value decomposition analysis. Chirality 2010;22:E186–E201.
62. Cubellis MV, Caillez F, Blundell TL, Lovell SC. Properties of polyproline II, a secondary structure element implicated in protein-protein interactions. Proteins 2005;58:880–882.

63. Whittington SJ, Chellgren BW, Hermann VM, Creamer TP. Urea promotes polyproline II helix formation: implications for denaturated states. Biochemistry 2005;44:6269–6275.
64. Yamamoto M, Nakagawa K, Ikeguchi M. Importance of polypeptide chain length for the correct local folding of a β-sheet protein. Biophys Chem 2012;168-169:40–47.
65. Jasanoff A, Fersht AR. Quantitative determination of helical propensities form trifluoroethanol titration curves. Biochemistry 1994;33:2129–2135.
66. Guttierrez-Cruz G, Van Heerden A, Wang K. Modular motif, structural folds and affinity profiles of PEVK segment of human fetal skeletal muscle titin. J Biol Chem 2001;276:7442–7449.
67. Makowska J, Rodziewicz-Motowidlo S, Baginska K, Vila JA, Liwo A, Chmurzynski L, Scheraga HA. Polyproline II conformation is one of many local conformational states and is not an overall conformation of unfolded peptides and proteins. Proc Natl Acad Sci U S A 2006;103:1744–1749.
68. Schubert M, Labudde D, Oschkinat H, Schmieder P. A software tool for the prediction of xaa-pro peptide bond formations in proteins based on 13C chemical shift statistic. J Biomol NMR 2002;24:149–154.
69. Kang YK. Puckering transition of proline residue in water. J Phys Chem B 2007; 111:10550–10556.
70. Cussac D, Frech M, Chardin P. Binding of the Grb2 SH2 domain to phosphotyrosine motifs does not change the affinity of its SH3 domains for Sos proline-rich motifs. EMBO J 1994;13:4011–4021.
71. Wittekind M, Mapelli C, Lee V, Goldfarb V, Friedrichs MS, Meyers CA, Mueller L. Solution structure of the Grb2 N-terminal SH3 domain complexed with a ten residue peptide derived from SOS: direct refinement against NOEs, *J*-couplings and ^{1}H and ^{13}C chemical shifts. J Mol Biol 1997;267:933–952.
72. Kohda D, Terasawa H, Ichikawa S, Ogura K, Hatanaka H, Mandiyan V, Ullrich A, Schlessinger J, Inagaki F. Solution structure and ligand-binding site of the carboxy-terminal SH3 Grb2. Curr Biol 1994;2:1029–1040.
73. Simon JA, Schreiber SL. Grb2 SH3 binding to peptides from Sos: evaluation of a general model for SH3-ligand interactions. Chem Biol 1995;2:53–60.
74. Cussac D, Vidal M, Leprince C, Liu WQ, Cornille F, Tiraboschi G, Roques BP, Garbay C. A Sos-derived peptidimer blocks the Ras signaling pathway by binding both Grb2 SH3 domains and displays antiproliferative activity. FASEB J 1999;13:31–38.
75. Jacquot Y, Broutin I, Miclet E, Nicaise M, Lequin O, Goasdoue N, Joss C, Karoyan P, Desmadril M, Ducruix A, Lavielle S. High affinity Grb2-SH3 domain ligand incorporating C^{β}-substituted prolines in a Sos-derived decapeptide. Bioorg Med Chem 2007;15:1439–1447.
76. Vidal M, Liu WQ, Lenoir C, Salzmann J, Gresh N, Garbay C. Design of peptoid analogue dimers and measure of their affinity for Grb2 SH3 domains. Biochemistry 2004;43:7336–7344.
77. Wang Y, Chen B, Li Y, Zhou D, Chen S. PNRC accumulates into the nucleolus by interaction with B23/nucleophosmin via its nucleolar localization sequence. Biochim Biophys Acta 2011;1813:109–119.
78. Zhou D, Zhong S, Ye JJ, Quach KM, Johnson DL, Chen S. PNRC is a unique nuclear receptor coactivator that stimulates RNA polymerase III-dependent transcription. J Mol Signal 2007:doi: 10.1186/1750-2187-2–5.
79. Hagarman A, Mathieu D, Toal S, Measey TJ, Schwalbe H, Schweitzer-Stenner R. Amino acids with hydrogen-bonding side chains have an intrinsic tendency to sample various turn conformations in aqueous solution. Chem Eur J 2011;17:6789–6797.
80. Woody RW. Studies of theoretical circular dichroism of polypeptides: Contributions of β turns. In: Blout ER, Bovey FA, Goodman M, Latan N editors. Peptides, polypeptides and proteins. New York: John Wiley & Sons;1974. p 338–350.
81. Rose GD, Gierasch LM, Smith JA. Turns in peptides and proteins. Adv Protein Chem 1985;37:1–109.
82. Bienkiewicz EA, Woody AYM, Woody RW. Conformation of the RNA polymerase II C-terminal domain: circular dichroism of long and short fragments. J Mol Biol 2000;297:119–133.
83. Moradi M, Babin V, Sagui C, Roland C. A statistical analysis of the PPII propensity of amino acid guests in proline-rich peptides. Biophys J 2011:100:1083–1093.
84. Yuzawa S, Yokochi M, Hatanaka H, Ogura K, Kataoka M, Miura KI, Mandiyan V, Schlessinger J, Inagaki F. Solution structure of Grb2 reveals extensive flexibility necessary for target recognition. J Mol Biol 2001;306:527–537.
85. Wang C, Pawley NH, Nicholson LK. The role of backbone motions in ligand binding to the c-Src SH3 domain. J Mol Biol 2001;313:873–887.
86. Dalgarno DC, Botfield MC, Rickles RJ. SH3 domains and drug design: ligands, structure and biological function. Biopolymer 1998;43:383–400.
87. Li SSC. Specificity and versatility of SH3 and other proline-recognition domains: structural basis and implications for cellular signal transduction. Biochem J 2005;390:641–653.
88. Feng S, Kasahara C, Rickles RJ, Schreiber SL. Specific interactions outside the proline-rich core of two classes of src homology 3 ligands. Proc Natl Acad Sci U S A 1995;92:12408–12415.
89. Bar-Sagi D. The Sos (Son of sevenless) protein. Trends Endocrinol Metab 1994;5:165–169.
90. Bourgoin-Voillard S, Gallo D, Laïos I, Cleeren A, El Bali L, Jacquot Y, Nonclercq D, Laurent G, Tabet JC, Leclercq G. Capacity of type I and II ligands to confer to estrogen receptor alpha an appropriate conformation for the recruitment of coactivators containing a LxxLL motif — Relationship with the regulation of receptor level and ERE-dependent transcription in MCF-7 cells. Biochem Pharmacol 2010;79:746–757.
91. Wärnmark A, Treuter E, Gustafsson JÅ, Hubbard RE, Brzozowski AM, Pike ACW. Intermediary factor 2 nuclear receptor box peptides with the coactivator binding site of estrogen receptor α. J Biol Chem 2002;277:21862–21868.